Molecular Cancer Therapeutics

Inhibition of mTORC2 Induces Cell-Cycle Arrest and Enhances the Cytotoxicity of Doxorubicin by Suppressing MDR1 Expression in HCC Cells

Bryan Wei Chen[1], Wei Chen[1], Hui Liang[1], Hao Liu[1], Chao Liang[1], Xiao Zhi[1], Li-qiang Hu[1], Xia-Zhen Yu[1], Tao Wei[1], Tao Ma[1], Fei Xue[2], Lei Zheng[3,4], Bin Zhao[5], Xin-Hua Feng[5], Xue-li Bai[1], and Ting-bo Liang[1,6]

Abstract

mTOR is aberrantly activated in hepatocellular carcinoma (HCC) and plays pivotal roles in tumorigenesis and chemoresistance. Rapamycin has been reported to exert antitumor activity in HCC and sensitizes HCC cells to cytotoxic agents. However, due to feedback activation of AKT after mTOR complex 1 (mTORC1) inhibition, simultaneous targeting of mTORC1/2 may be more effective. In this study, we examined the interaction between the dual mTORC1/2 inhibitor OSI-027 and doxorubicin *in vitro* and *in vivo*. OSI-027 was found to reduce phosphorylation of both mTORC1 and mTORC2 substrates, including 4E-BP1, p70S6K, and AKT (Ser473), and inhibit HCC cell proliferation. Similar to OSI-027 treatment, knockdown of *mTORC2* induced G_0–G_1 phase cell-cycle arrest. In contrast, rapamycin or knockdown of *mTORC1* increased phosphorylation of AKT (Ser473), yet had little antiproliferative effect. Notably, OSI-027 synergized with doxorubicin for the antiproliferative efficacy in a manner dependent of MDR1 expression in HCC cells. The synergistic antitumor effect of OSI-027 and doxorubicin was also observed in a HCC xenograft mouse model. Moreover, AKT was required for OSI-027–induced cell-cycle arrest and downregulation of MDR1. Our findings provide a rationale for dual mTORC1/mTORC2 inhibitors, such as OSI-027, as monotherapy or in combination with cytotoxic agents to treat HCC. *Mol Cancer Ther; 14(8); 1805–15. ©2015 AACR.*

Introduction

Hepatocellular carcinoma (HCC) is the fifth most common type of cancer and second leading cause of cancer-related deaths worldwide (1). Surgery is often unsuitable in advanced disease, although surgical resection or liver transplantations are suitable therapeutic approaches for early-stage HCC (2). Doxorubicin is widely used to treat HCC (3, 4), despite the fact that monotherapies such as doxorubicin have shown limited efficacy in clinical trials (2, 4, 5). Thus, research into novel effective chemotherapeutic strategies continues; combination therapy based on traditional chemotherapeutic agents and small-molecule inhibitors that selectively target cancer cells represents a potentially promising approach.

The mammalian target of rapamycin (mTOR) is a critical mediator of numerous cellular signals in oncogenesis (6). The mTOR complex is comprised of two distinct components: mTORC1 and mTORC2. Rapamycin-sensitive mTORC1 directly targets ribosomal protein S6 kinase (p70S6K) and eukaryotic translation initiation factor 4E-binding protein 1 (4E-BP1) to promote cap-dependent protein translation (7, 8). Rapamycin-insensitive mTORC2 phosphorylates the hydrophobic motif (Ser473) of the prosurvival kinase AKT, which subsequently facilitates autophosphorylation of AKT on Thr308 to maximize AKT activity (9). Hyperactivation of AKT promotes cell growth, proliferation, and survival and inhibits apoptosis (10, 11). At molecular level, Ser2448 and Ser2481 are two of the most studied phosphorylation sites on mTOR. Recent studies have demonstrated that mTORC1 contains mTOR phosphorylated predominantly on S2448, whereas mTORC2 contains mTOR on S2481. Moreover, phosphorylation of mTOR on 2448 is a biomarker of mTORC1 activity, whereas phosphorylation of the protein on Ser2481 represents mTORC2 activity (12).

MTOR is aberrantly activated in human HCC (13) and plays a pivotal role in HCC tumorigenesis (14). Targeting mTOR using rapamycin can sensitize tumor cells to cisplatin (15), doxorubicin (16), and other targeted therapeutic agents such as histone deacetylase inhibitors (17). However, mTORC1 inhibition activates mTORC2 signaling via disengaging the p70S6K-define (IRS) negative feedback loop, thus limiting the antitumor efficacy of

[1]Department of Hepatobiliary and Pancreatic Surgery, The Second Affiliated Hospital, Zhejiang University School of Medicine, Hangzhou, Zhejiang, China. [2]Department of Hepatobiliary and Pancreatic Surgery, People's Hospital of Zhengzhou University/Henan Provincial People's Hospital, Zhengzhou, Henan, China. [3]Department of Oncology, Johns Hopkins University School of Medicine, Baltimore, Maryland. [4]Sidney Kimmel Cancer Center, Johns Hopkins University School of Medicine, Baltimore, Maryland. [5]Life Sciences Institute and Innovation Center for Cell Signaling Network, Zhejiang University, Hangzhou, Zhejiang, China. [6]Collaborative Innovation Center for Cancer Medicine, Zhejiang University, Hangzhou, Zhejiang, China.

Note: Supplementary data for this article are available at Molecular Cancer Therapeutics Online (http://mct.aacrjournals.org/).

B.W. Chen, W. Chen, and H. Liang contributed equally to this article.

Corresponding Author: Ting-bo Liang, Department of Hepatobiliary and Pancreatic Surgery, The Second Affiliated Hospital, Zhejiang University School of Medicine, 88 Jiefang Road, Hangzhou 310009, China. Phone and Fax: 86-571-87315006; E-mail: liangtingbo@zju.edu.cn

doi: 10.1158/1535-7163.MCT-15-0029

this strategy (18). Therefore, efforts are now underway to identify a mechanism of targeting mTORC2 in cancer.

OSI-027, a novel ATP-competitive inhibitor of mTOR, inhibits both components of the mTOR complex and has demonstrated potent anticancer effects in colorectal cancer, breast cancer, and lymphoma (19–21). However, OSI-027 has been reported to enhance the cytotoxicity of cisplatin and EGFR inhibitor (EGFRi) in breast cancer and head/neck squamous cell carcinoma, respectively (22, 23). Given that rapamycin and rapalog (RAD001) exert additive antitumor effects when administered with doxorubicin in preclinical models of HCC (16, 24), we investigated the antitumor effect of OSI-027 alone and in combination with doxorubicin. In the present study, we demonstrate that inhibition of mTORC2, but not mTORC1, abrogated hyperactivation of AKT and consequently promoted cell-cycle arrest in a panel of HCC lines. Furthermore, inhibition of mTORC2 potently sensitized HCC cancer cells to doxorubicin both *in vitro* and *in vivo*. This study provides a rationale for the use of dual mTORC1/mTORC2 inhibitors as a monotherapy or in combination with traditional chemotherapeutic agents for the treatment of HCC.

Materials and Methods

Cell lines and cell culture

Human HCC cell lines and HL-7702 cells were obtained from Shanghai Institute for Biological Sciences, China on February 10, 2012. Huh-7 and SK-Hep1 cells were cultured in high glucose DMEM (Gibco) supplemented with 10% FBS (Gibco) and 1% penicillin/streptomycin (Sigma-Aldrich); Hep3B cells, MEM (Gibco) supplemented with 10% FBS and 1% penicillin/streptomycin; SNU387, SNU-449, and HL-7702 cells, RPMI-1640 (Gibco) supplemented with 10% FBS and 1% penicillin/streptomycin. Cells were maintained at 37°C in a humidified incubator with 5% CO_2 and were used within 3 months of resuscitation. We have had all the cell lines authenticated by a professional biotechnology company in 2014.

Reagents

OSI-027 and GSK690693 were purchased from Selleck; rapamycin, doxorubicin, MG-132, and cycloheximide (CHX) from Sigma-Aldrich. Stock solutions were prepared in dimethyl sulfoxide (DMSO; Sigma-Aldrich), stored at −20°C, and diluted in fresh medium for each experiment. The final concentration of DMSO did not exceed 0.5% in any experiment.

Cell viability and proliferation assays

To evaluate relative cell viability, HCC cells (5,000 per well) were seeded into 96-well microplates, incubated overnight, the culture medium was replaced with complete media containing diverse concentrations of rapamycin (0.1, 0.4, 1.6, 6.4, 25.6, 102.4, and 409.6 μmol/L) or OSI-027 (0.3125, 0.625, 1.25, 2.5, 5.0, 10, and 20 μmol/L) for 48 hours, then the cell counting kit-8 assay (CCK-8; KeyGEN) was conducted following the manufacturer's instructions. The dosages of OSI-027 to treat HL-7702 cells were 0.25, 0.50, 1.0, 2.0, 4.0, 8.0, and 16 μmol/L. Cell viability was expressed relative to untreated control cells.

To evaluate cell proliferation, SNU-387 cells were treated with 10 μmol/L rapamycin or 2.0, 5.0, and 10 μmol/L OSI-027, respectively, while other four cell lines were incubated with 2.0 μmol/L rapamycin or indicated concentrations of OSI-027 (0.5, 1.0, 2.0 μmol/L). Then cells were assayed using the Click-iT 5-ethynyl-20-deoxyuridine (EdU) Imaging Kit (Invitrogen) following the manufacturer's instructions and counterstained with Hoechst 33342. The percentage of proliferating cells in five random fields of view per slide was determined under an inverted fluorescence microscope (Olympus) and expressed relative to untreated control cells.

Apoptosis and cell-cycle analysis

Cells were treated with OSI-027 (5.0, 10, and 20 μmol/L for SNU-387 cells, 1.0, 2.0, and 4.0 μmol/L for other four HCC cell lines) for 48 hours, stained using the Annexin V-PE/7AAD apoptosis kit (BD Biosciences) according to the manufacturer's protocol, and analyzed using a BD FACS Caliber flow cytometer using BD Cell Quest software.

For cell-cycle analysis, cells were treated with DMSO, rapamycin (20 μmol/L for SNU-387 and 4 μmol/L for other four HCC cell lines) or OSI-027 as described for apoptosis assay for 48 hours, stained with propidium iodide (PI; Dawen) and analyzed by flow cytometry. Quantitative cell-cycle analysis was conducted using ModFit software (Verity Software House). Cell proliferation was expressed as the percentage of S + G_2–M phase cells (25).

Drug combination analysis

Multiple drug-effect analysis was used to evaluate the effects of combined drug treatment, as described by Chou and Talalay (26). The results of the CCK-8 assay were calculated using the following equation: combination index (CI) = $(D)1/(Dx)1 + (D)2/(Dx)2$, where $(Dx)1$ and $(Dx)2$ are the concentrations of drug 1 and drug 2 alone that achieve effect f_a; $(D)1$ and $(D)2$ are the concentrations of drug 1 and drug 2 in combination that give the same effect f_a. A CI < 1 indicates synergism; CI = 1 and CI > 1 indicate an additive effect and antagonism, respectively.

RNAi

Human siRNAs specific for *Raptor* and *Rictor* were synthesized by GenePharma Co., Ltd. Detailed information of *Raptor* and *Rictor* siRNAs is described in the Supplementary Materials and Methods. *MDR1*, *mTOR*, and *AKT*-specific siRNAs were purchased from Cell Signaling Technology. Cells were transfected with siRNAs using Roche X-tremeGENE 9 (Roche Applied Science) following the manufacturer's instructions. Transfection medium was replaced with complete medium 6 hours later, and efficiency of siRNA knockdown was confirmed by immunoblotting.

Quantitative real-time PCR

Cells were treated with DMSO, OSI-027 (double the IC_{50} concentrations), doxorubicin (IC_{50} concentrations), or OSI-027 plus doxorubicin for 24 hours, and total RNA was extracted using TRIzol Reagent (Invitrogen) and reverse transcribed using the Prime Script reagent RT Kit (Takara Biotechnology). Primers for *MDR1* were designed and purchased from Takara. PCR was performed on an ABI Prism 7900HT Real-Time System (Applied Biosystems Inc). *MDR1* mRNA expression was normalized to *β-actin* and determined using the comparative $2^{-\Delta\Delta Ct}$ method (27). Detailed sequences of primers for *MDR1* and *β-actin* are given in the Supplementary Materials and Methods.

Immunoblotting

Immunoblotting was performed using standard protocols. Briefly, 20 μg protein lysates were fractionated on 8% to 12% Tris-glycine polyacrylamide gels, transferred to polyvinylidene

difluoride membranes, blocked, incubated overnight with primary antibodies (all 1:1,000 dilution) followed by the appropriate horseradish peroxidase (HRP)-conjugated secondary antibody (1:2,000 dilution), and developed using enhanced chemiluminescence. All antibodies were obtained from Cell Signaling Technology, with the exception of anti-Cyclin D1 (Epitomics) and the HRP-conjugated secondary antibodies (Beyotime Institute of Biotechnology).

Xenograft study

Male athymic nude mice (3–4 week old; 18–20 g) were purchased from Shanghai Experimental Animal Centre and housed in a specific pathogen-free facility. Animal care was in compliance with the guidelines of the Animal Ethics Committee of Zhejiang University. Mice were inoculated subcutaneously in the left flank with 10^6 Huh-7 cells in 100 μL saline solution.

Two weeks after tumor inoculation, twenty tumor-bearing mice were divided into four groups ($n = 5$ each): control group; OSI-027 group [orally administered 30 mg/kg OSI-027 in 20% Trappsol [(CTD Holdings Inc)] every other day; doxorubicin group, injected via the caudal vein with 2 mg/kg doxorubicin in saline solution every other day; and combination group, administered 30 mg/kg OSI-027 and 2 mg/kg doxorubicin every other day. Tumor volume and body weight were measured every 2 days. Tumor volume was calculated using $(L \times W^2)/2$, where L is the diameter of the longest dimension and W is the orthogonal diameter. Relative tumor volume (RTV) was calculated using V_t/V_0, where V_t is the tumor volume of all the groups at indicated time t and V_0 is the original tumor volume of the animals. After 2 weeks, the mice were euthanized by cervical dislocation. Tumor growth inhibition (TGI%) was calculated using $\{1-[(T_t/T_0)/(C_t/C_0)]/1-[C_0/C_t]\} \times 100$, where T_t is the tumor volume of the treated group at indicated time t, T_0 is the original tumor volume of the treated animal, C_t is median tumor volume of untreated mice at time t, and C_0 is the median original tumor volume of the control group.

Results

OSI-027 inhibits the growth of HCC cells in a concentration-dependent manner *in vitro*

In agreement with a previous study (28), the CCK-8 assay demonstrated rapamycin hardly had any cytotoxicity (IC_{50} > 100 mmol/L) in all HCC cell lines tested (Fig. 1A). In contrast, the cytotoxicity of OSI-027 varied in HCC cell lines, with IC_{50} values ranging from 1 to 8 μmol/L (Fig. 1B; Table 1). Moreover, OSI-027 had a lower cytotoxicity in HL-7702 normal human liver cells (IC_{50} > 25 μmol/L) than HCC cells (Fig. 1C).

As the CCK-8 assay cannot distinguish between cell-cycle arrest and cytotoxicity in continuously cycling cell lines, we used the EdU thymidine analog incorporation assay (29) to estimate proliferation in HCC cells treated with rapamycin or OSI-027 for 48 hours. Consistent with the CCK-8 assay, rapamycin did not significantly affect HCC cell proliferation, whereas OSI-027 significantly inhibited HCC cell proliferation in a dose-dependent manner (Fig. 1D and E and Supplementary Fig. S1A–S1C).

OSI-027, but not rapamycin, inhibits both the mTORC1 and mTORC2 signaling cascades in HCC cells

We investigated the mechanism underlying the increased cytotoxicity of OSI-027 compared with rapamycin (Fig. 1). Immunoblotting demonstrated ubiquitous basal activation of mTOR-dependent signaling in HCC cells, as indicated by high levels of phosphorylated mTOR substrates (Fig. 2A). Exposure of HCC cells to OSI-027 for 8 hours completely inhibited phosphorylation of mTOR on Ser2481, the marker of mTORC2 complex activity, and its substrate AKT (Ser473) in a dose-dependent fashion. In contrast, rapamycin inhibited mTORC1 activity (phosphorylation of Ser2448) without affecting mTOR2 activity (Ser2481), and also markedly increased AKT phosphorylation (Ser473; Fig. 2B–F; lanes 1, 2, 4). OSI-027 inhibited the phosphorylation of all mTORC1 substrates examined, including 4E-BP1 (Thr37/46) and p70S6K (Thr389). In contrast, rapamycin inhibited phosphorylation of p70S6K, but not 4E-BP1 (Fig. 2B–F; lanes 6, 8). Therefore, OSI-027 efficiently inhibits both the mTORC1 and mTORC2 signaling cascades in HCC cells, whereas ramamycin partially inhibits mTORC1 but does not inhibit mTORC2, even at relatively high doses in the micromolar range. These results are consistent with previous studies on rapamycin (30, 31) and may explain the poor efficacy of rapamycin *in vitro*.

OSI-027, but not rapamycin, induces cell-cycle arrest in HCC cells

Considering the significance of mTOR in the regulation of cell metabolism, cell-cycle progression and survival (32–35), we investigated the antiproliferative effect of OSI-027 further. Annexin V staining and flow cytometry demonstrated treatment with OSI-027 for 48 hours (Supplementary Fig. S2A and S2B) did not induce apoptosis, as previously reported (19, 21, 36). Nevertheless, OSI-027 increased the proportion of SNU-449 cells in the G_0–G_1 phase (from 67.29% to 89.31%) in a dose-dependent manner (Fig. 3A). In contrast, rapamycin did not significantly affect the G_0–G_1 ratio compared with DMSO control-treated cells (Fig. 3A). Similar results were obtained in the other four HCC cell lines, except for SNU-387 cells in which rapamycin induced a low level of cell-cycle arrest (Fig. 3A and Supplementary Fig. S3A–S3C). In agreement with the cell-cycle distribution analysis, OSI-027 significantly reduced the expression of Cyclin D1 and CDK4 in all five HCC cell lines, whereas rapamycin did not significantly affect the expression of these cell cycle-associated proteins (Fig. 3B and Supplementary Fig. S 3D).

Targeting of mTORC2, rather than mTORC1, promotes G_0–G_1-phase arrest in HCC cell lines

To further identify whether mTORC1 or mTORC2 participates in the induction of cell-cycle arrest by OSI-027, the effects of Raptor, Rictor, and mTOR on cell-cycle progression were examined. Raptor is short for regulatory-associated protein of mTOR and regarded as one of the components of mTORC1. Raptor serves as a binding platform where substrates are presented to mTOR for subsequent activation of mTORC1 (37). As for rapamycin-insensitive companion of mTOR (Rictor), it contributes to the structural foundation of mTORC2. And in the absence of Rictor, mTORC2 becomes inactive (38). Knockdown of *Rictor* or *mTOR* clearly increased the number of G_0–G_1 phase cells in all HCC cell lines tested, whereas knockdown of *Raptor* had no significant effect (Fig. 3C and D and Supplementary Fig. S4A–S4C). Furthermore, knockdown of *Rictor* or *mTOR*, but not *Raptor*, simultaneously reduced Cyclin D1 expression and AKT phosphorylation (Ser473) in Hep-3B and SNU-449 cells (Fig. 3E; lanes 4, 5). Knockdown of *Raptor* even slightly increased AKT phosphorylation (Ser473; Fig. 3E; lane 4), consistent with activation of AKT

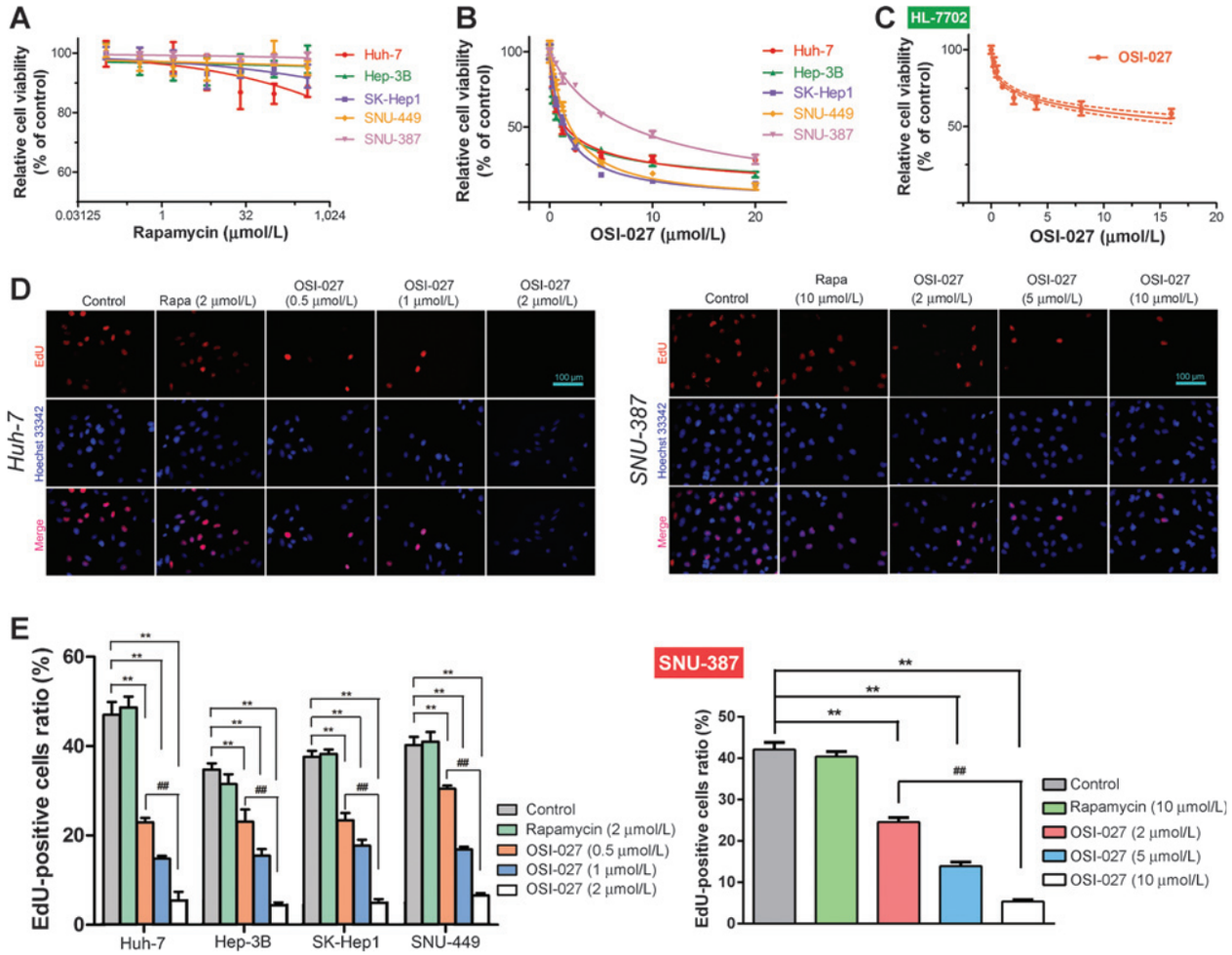

Figure 1.
Effect of rapamycin and OSI-027 on HCC cell proliferation. A and B, mean ± SD relative viability of a panel of HCC cells after treatment with various concentrations of rapamycin (A) or OSI-027 (B) for 48 hours. C, mean ± SD relative viability of HL-7702 cells treated with various concentrations of OSI-027 for 48 hours. D and E, EdU staining (D) and relative EdU-positive cell ratios (E) for HCC cells treated with indicated concentration of rapamycin (Rapa) or various concentrations of OSI-027 for 48 hours; ** and ## $P < 0.01$, one-way ANOVA.

by rapamycin (Fig. 2B–F). These data suggest that targeting of mTORC2, but not mTORC1, promotes G_0–G_1-phase arrest and phosphorylation of the hydrophobic motif of AKT may be required to maintain Cyclin D1 expression and promote cell-cycle progression in HCC cells.

OSI-027 synergistically enhances the efficacy of doxorubicin via reversing doxorubicin-induced upregulation of MDR1

Multidrug resistance protein 1(MDR1) plays a role in the doxorubicin resistance of HCC cell lines (39). Given that marked downregulation of MDR1 was observed in *Rictor*-silenced HCC

Table 1. IC_{50} values and statistical analyses of OSI-027 and doxorubicin (DOX) treatments in HCC cell lines and HL-7702

	IC_{50} (μmol/L)[a]			
HCC cell lines	**OSI-027**	**DOX**	**OSI-027+DOX**	**Combination index**
Huh-7	1.613 (1.445–1.782)	0.6490 (0.5959–0.7022)	OSI 0.3857 (0.3685–0.4028) DOX 0.3857 (0.3685–0.4028)	0.8333
Hep-3B	1.051 (0.8065–1.295)	1.157 (1.107–1.206)	OSI 0.3551 (0.2977–0.4125) DOX 0.3551 (0.2977–0.4125)	0.6448
SK-Hep1	1.303 (1.175–1.432)	0.6720 (0.6133–0.7306)	OSI 0.7423 (0.6870–0.7977) DOX 0.1485 (0.1374–0.1595)	0.7907
SNU-449	2.063 (1.975–2.150)	1.964 (1.831–2.098)	OSI 0.05758 (0.04519–0.06997) DOX 1.152 (1.052–1.252)	0.6145
SNU-387	8.728 (7.486–9.969)	1.063 (0.9927–1.134)	OSI 0.9397 (0.8569–1.023) DOX 0.4696 (0.4363–0.5029)	0.5494
HL-7702	26.07 (16.85–35.30)	/	/	/

[a]IC_{50} values show OSI-027 and doxorubicin concentration [μmol/L, mean (95% confidence intervals)].

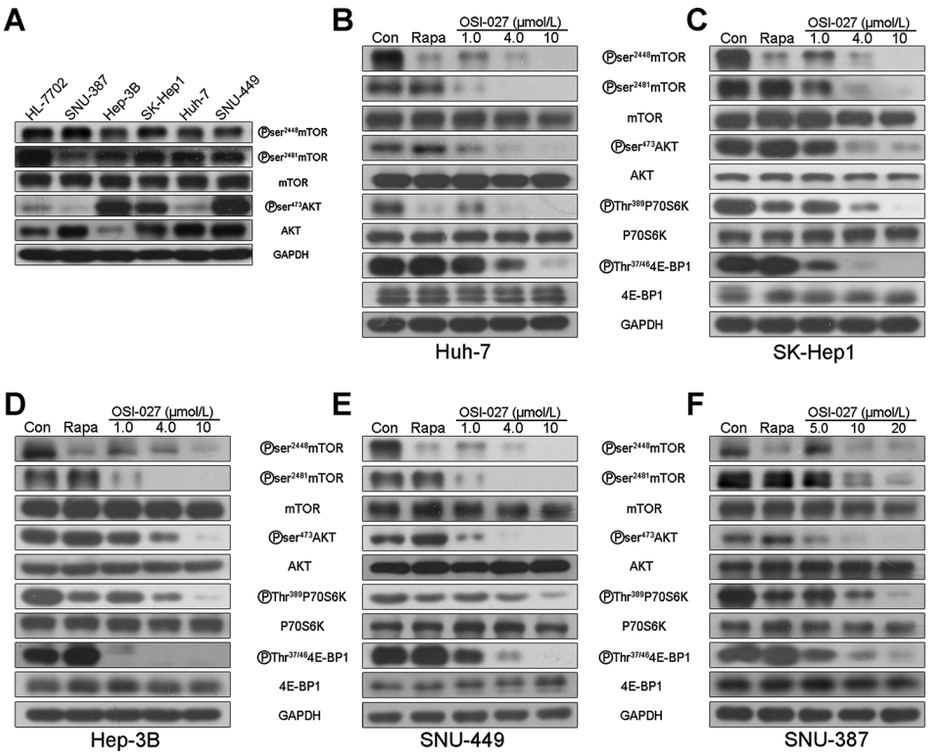

Figure 2.
OSI-027 blocks mTORC1/C2 signaling more efficiently than rapamycin. A, immunoblot analysis of basal mTORC1 and mTORC2 signaling in representative HCC cells and HL-7702 cells. GAPDH was used as a protein loading control. B–F, immunoblot analysis of mTORC1 and mTORC2 signaling in (B) Huh-7, (C) SK-Hep1, (D) Hep-3B, and (E) SNU-449 cells treated with 4 μmol/L rapamycin (Rapa) or various concentrations of OSI-027 for 8 hours, and (F) SNU-387 cells treated with 10 μmol/L rapamycin or various concentrations of OSI-027 for 8 hours.

cells (Fig. 3E; lane 6), we examined whether the combination of OSI-027 and doxorubicin led to an additive or synergistic effect. Drug combination index (CI) analysis is a generalized method for analyzing the effects of multiple drugs and identifying addition, synergism, and antagonism. We treated HCC cells with decreasing half-log concentrations of OSI-027, doxorubicin, or a combination of both. The CCK-8 assay was performed and the data were analyzed using method of Chou and Talalay, as described in Materials and Methods. The dose-response curves demonstrated the combined treatment resulted in an enhanced, synergistic effect (CI values ranging from 0.5494 to 0.8333; Fig. 4A; Table 1). Immunoblotting demonstrated downregulation of MDR1 when the cells were treated with approximately double the IC_{50} concentrations of OSI-027 for 24 h (Fig. 4B). Moreover, upregulation of MDR1 induced by doxorubicin could be reversed by the dual mTORC1/mTORC2 inhibitor OSI-027 (Fig. 4B), especially in Huh-7 and Hep-3B cells. Real-time qRT-PCR confirmed the Western blotting results; the relative expression of *MDR1* mRNA reduced by approximately half in OSI-027–treated cells (except in SK-Hep1 cells; Fig. 4C). Furthermore, OSI-027 potently reversed the high levels of *MDR1* mRNA expression induced by doxorubicin (Fig. 4C).

Next, we investigated how OSI-027 affects MDR1 expression. As the ubiquitin-proteasome pathway regulates degradation of MDR1 in mammalian cells (40), we treated the cells with a proteasome inhibitor (MG132) alone or combination with OSI-027. MG132 increased the levels of MDR1 in HCC cells, and this effect could be reversed by OSI-027 (Fig. 4D, a). However, no further reduction MDR1 expression was obtained when the cells were treated with a combination of cycloheximide and OSI-027 compared with cycloheximide alone (Fig. 4D, b). Therefore, OSI-027 downregulates MDR1 by inhibiting its synthesis rather than promoting its degradation.

Hep-3B cells were transfected with negative control (NC) siRNA or *MDR1* siRNA and subjected to the CCK-8 assay to confirm whether MDR1 is involved in the synergistic effect of OSI-027 and doxorubicin. Knockdown of *MDR1* sensitized Hep-3B cells to doxorubicin (IC_{50} values reduced from 2.016 μmol/L to 0.4886 μmol/L), without affecting the sensitivity of the cells to OSI-027 (Table 2 and Supplementary Fig. S5A). Correspondingly, the dose-response graphs indicated that knockdown of *MDR1* attenuated the synergistic effect of OSI-027 and doxorubicin (Fig. 4F); this observation was supported by an increase in the CI values (Table 2). Similar results were observed in SNU-449 cells (Supplementary Fig. S5B–S5D).

Taken together, OSI-027 reverses the high levels of MDR1 expression induced by doxorubicin via inhibiting the synthesis of MDR1, and consequently synergizes the efficacy of doxorubicin *in vitro*.

The combination of OSI-027 and doxorubicin significantly enhances tumor growth inhibition in HCC *in vivo*

OSI-027 inhibits tumor growth more effectively than rapamycin in a number of *in vivo* cancer models, including colorectal cancer, breast cancer and lymphoma (19–21). Other studies have reported a potent reduction in the tumor burden in mice bearing HCC xenografts treated with a combination of doxorubicin plus rapamycin or rapalog (16, 24). Given the potent synergistic effect of mTORC1/mTORC2 inhibition in combination with doxorubicin *in vitro*, we assessed the effects of this combination *in vivo*. Nude mice were inoculated with a representative HCC cell line, Huh-7, and randomized to one of four treatment groups (control, OSI-027 alone, doxorubicin alone, or OSI-027 plus doxorubicin).

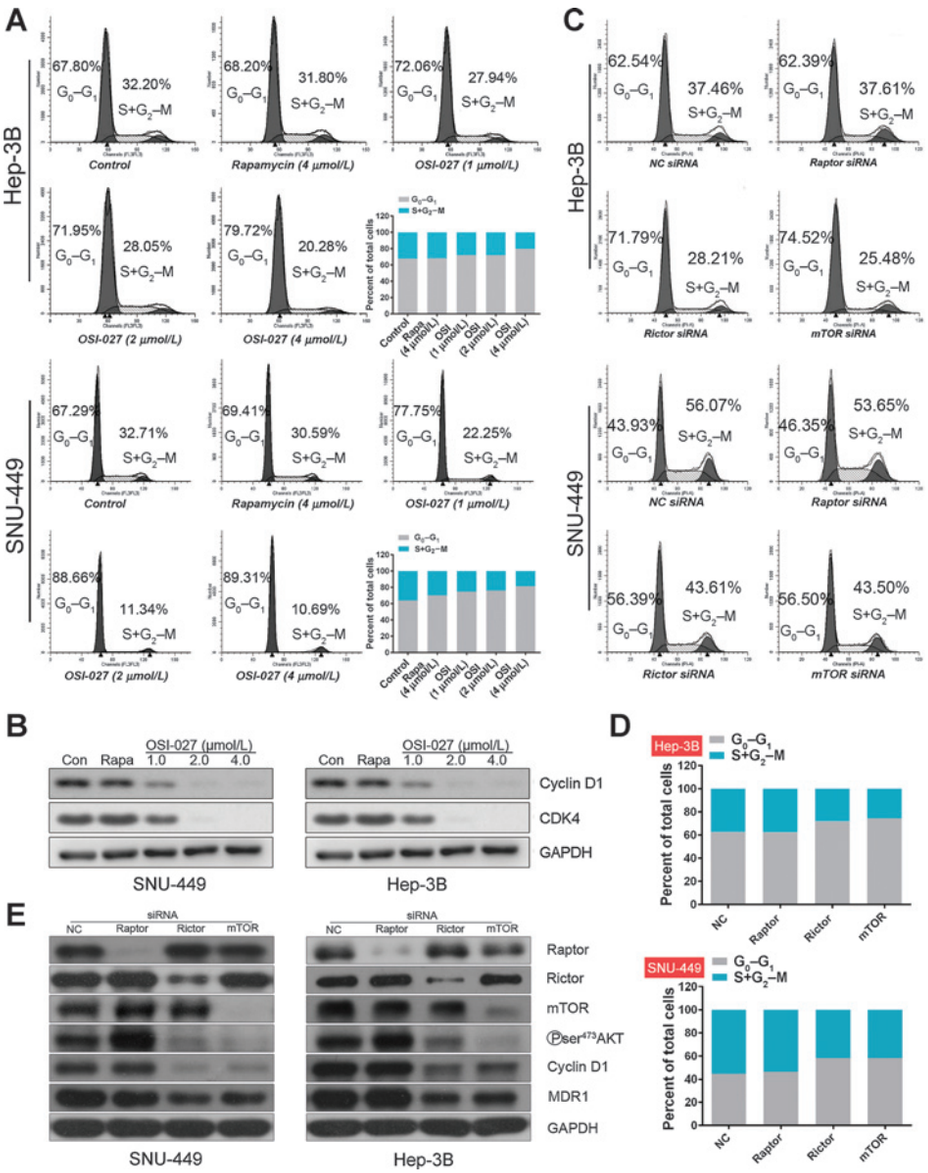

Figure 3.
Effect of rapamycin and OSI-027 on HCC cell-cycle progression (A and B), and knockdown of *Rictor* or *mTOR*, but not *Raptor*, results in cell-cycle arrest (C–E). A, flow-cytometric analysis of cell-cycle distribution in Hep-3B and SNU-449 cells treated with 4 μmol/L rapamycin (Rapa) or the indicated concentrations of OSI-027 (OSI) for 48 hours. B, Western blot analysis of Cyclin D1 and CDK4 in HCC cells treated with rapamycin or OSI-027. GAPDH was used as a protein loading control. C–E, HCC cells were transfected with 50 nmol/L of siRNA against *Raptor*, *Rictor*, *mTOR*, or negative control (NC) siRNA as indicated, and incubated for 48 hours. Flow-cytometric analysis (C) and quantification of cell-cycle distribution (D) for Hep-3B and SNU-449 cells. E, immunoblot analysis of Raptor, Rictor, mTOR, p-AKT (S473), Cyclin D1, MDR1, and GAPDH (loading control) in Hep-3B cells and SNU-499 cells. These experiments were repeated three times with similar results.

Tumor growth was significantly delayed in the group receiving both OSI-027 plus doxorubicin compared with either treatment alone or the vehicle control (Fig. 5A and B), indicative of a synergistic effect. In comparison with monotherapy, the combination of OSI-027 plus doxorubicin increased the relative tumor-inhibitory rate from approximately 55% to 80.11% (Fig. 5C). Interestingly, OSI-027 alone exhibited a similar antitumor efficacy to doxorubicin, the typical chemotherapeutic drug for HCC, with no significant difference between the tumor volumes or tumor-inhibitory rate of these groups (Fig. 5B and C).

OSI-027 was well tolerated using this schedule, with no animals requiring euthanasia for severe weight loss or signs of other toxicities, though the mice receiving OSI-027 did experience modest weight loss. Moreover, the combination of OSI-027 plus doxorubicin did not result in additive toxicity compared with either treatment alone (Fig. 5D).

Cell-cycle arrest induced by targeting mTORC2 and the reversal of MDR1 expression induced by OSI-027 are both AKT dependent

Given that the downregulation of Cyclin D1/CDK4 and MDR1 coincided with decreased AKT phosphorylation (Ser473), we examined the role of AKT in these processes. As expected, knockdown of *AKT* using a siRNA resulted a robust reduction in AKT phosphorylation (Ser473) and simultaneously downregulated Cyclin D1 (Fig. 6A). Flow cytometry revealed induction of G_0–G_1-phase arrest after knockdown of *AKT* in the four HCC cell lines tested compared with NC siRNA-transfected cells (Fig. 6B and C and Supplementary Fig. S6A–S6C); this effect was almost of the same magnitude as the G_0–G_1-phase arrest induced by knockdown of *Rictor*/*mTOR* (Fig. 3A). Knockdown of *AKT* also markedly downregulated MDR1 (Fig. 6A). Therefore, the cell-cycle arrest, downregulation of Cyclin D1, and reversal of MDR1 expression

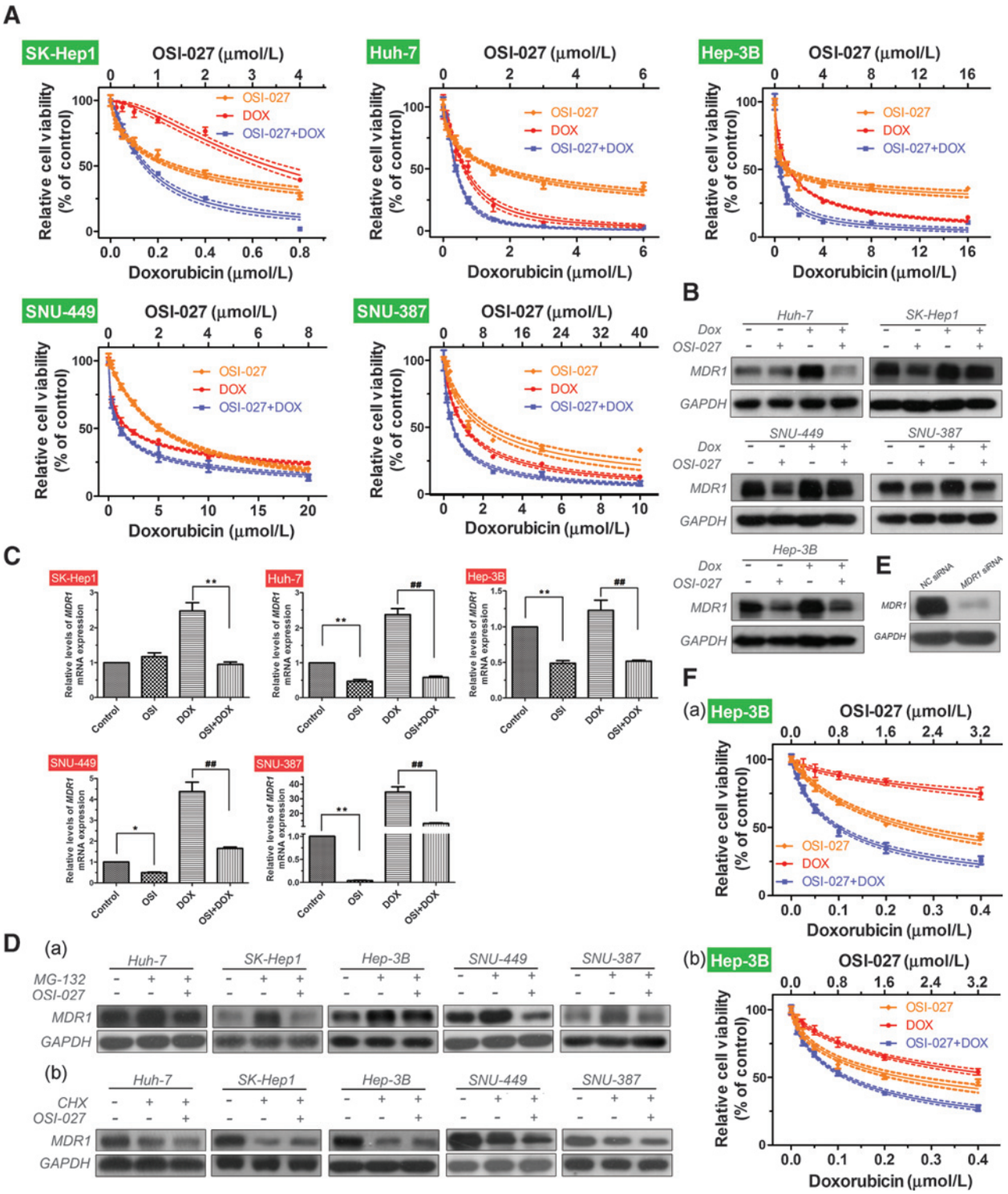

Figure 4.
OSI-027 synergizes the efficacy of doxorubicin via reversing the upregulation of MDR1 induced by doxorubicin. A, dose-response curves for HCC cells treated with OSI-027, doxorubicin, or a combination of both for 48 hours. Immunoblotting analysis (B) and RT-PCR analysis of MDR1 expression (C) in HCC cells treated with OSI-027 (OSI, double the IC_{50} concentrations for each cell line), doxorubicin (IC_{50} concentrations), or a combination of both for 24 hours. GAPDH was used as a protein loading control. *, $P < 0.05$; ** and ##, $P < 0.01$, one-way ANOVA D, immunoblotting analysis of MDR1 in HCC cells treated with (a) 1 μmol/L MG-132 or (b) 100 μg/mL cycloheximide (CHX) in the presence or absence of OSI-027 (double the IC_{50} concentrations) for 24 hours. E, immunoblotting analysis of the efficiency of *MDR1* siRNA-mediated knockdown compared to control cells (NC). F, dose-effect curves for OSI-027, doxorubicin, and the combination of both drugs in (a) control cells and (b) *MDR1*-knockdown Hep-3B cells at 48 hours.

Table 2. IC_{50} values and statistical analyses of OSI-027 and doxorubicin treatments in *MDR1* knockdown HCC cell lines

HCC cell lines (Treatment)	IC_{50} (μmol/L)[a]			
	OSI-027	DOX	OSI-027+DOX	Combination index
Hep-3B (NC siRNA)	2.041 (1.849–2.233)	2.016 (0.9769–3.056)	OSI 0.7953 (0.7377–0.8530) DOX 0.09942 (0.09221–0.1066)	0.4390
Hep-3B (*MDR1* siRNA)	1.915 (1.641–2.189)	0.4886 (0.4203–0.5569)	OSI 0.9442 (0.8816–1.007) DOX 0.1180 (0.1102–0.1259)	0.8164
SNU-449 (NC siRNA)	2.751 (1.702–3.799)	3.520 (3.090–3.949)	OSI 0.4973 (0.4534–0.5413) DOX 1.989 (1.813–2.165)	0.4694
SNU-449 (*MDR1* siRNA)	2.511 (1.603–3.419)	1.845 (1.702–1.988)	OSI 0.1829 (0.1668–0.1990) DOX 0.7317 (0.6673–0.7961)	0.7458

[a]IC_{50} values show OSI-027 and doxorubicin concentration [μmol/L, mean (95% confidence intervals)].

induced by inhibition of mTORC2 using OSI-027 are AKT dependent.

Discussion

As a crucial component of the PI3K/AKT pathway that plays a critical role in oncogenesis, mTOR is aberrantly activated in most types of cancer, including human HCC. Increased expression of total p70S6K correlated with activation of mTOR in almost half of patients with HCC (33 out of 73; ref. 13). Consistent with the early study, we found that mTOR and p-mTOR were both overexpressed in either tumor or peritumor tissue compared with normal liver tissue in 60% of the patients detected, indicating the activation of mTOR in HCC (Supplementary Fig. S7). In addition, chromosomal gains in Rictor and positive p-RPS6 staining correlated with tumor recurrence in a larger cohort of patients with HCC (14). In this study, we observed that, though OSI-027 also targets mTORC1, OSI-027 inhibited proliferation and promoted cell-cycle arrest via inhibition of mTORC2, suggesting that mTORC2 plays a critical role in the maintenance of cell viability. We also demonstrated that by inhibiting both mTORC1 and mTORC2, OSI-027 may outperform rapamycin as an anticancer agent. Moreover, OSI-027 exerted a synergistic antitumor effect when combined with doxorubicin. Taken together, this study offers a rationale for clinical testing of mTORC1/mTORC2 inhibitors as monotherapy or concurrently with doxorubicin.

Rapalogs have displayed significant antitumor activity in renal cell carcinoma (41) and have been approved by the U.S. Food and Drug Administration for clinical use. We previously demonstrated that inhibition of mTOR using rapamycin delayed HCC xenograft tumor growth *in vivo* (42). However, we here found that rapamycin hardly exerted an anticancer effect in HCC *in vitro* (Fig. 1A and D). These seemingly contradictory findings can be explained by the different microenvironments of *in vitro* experiments and rodent xenograft models. Inhibition

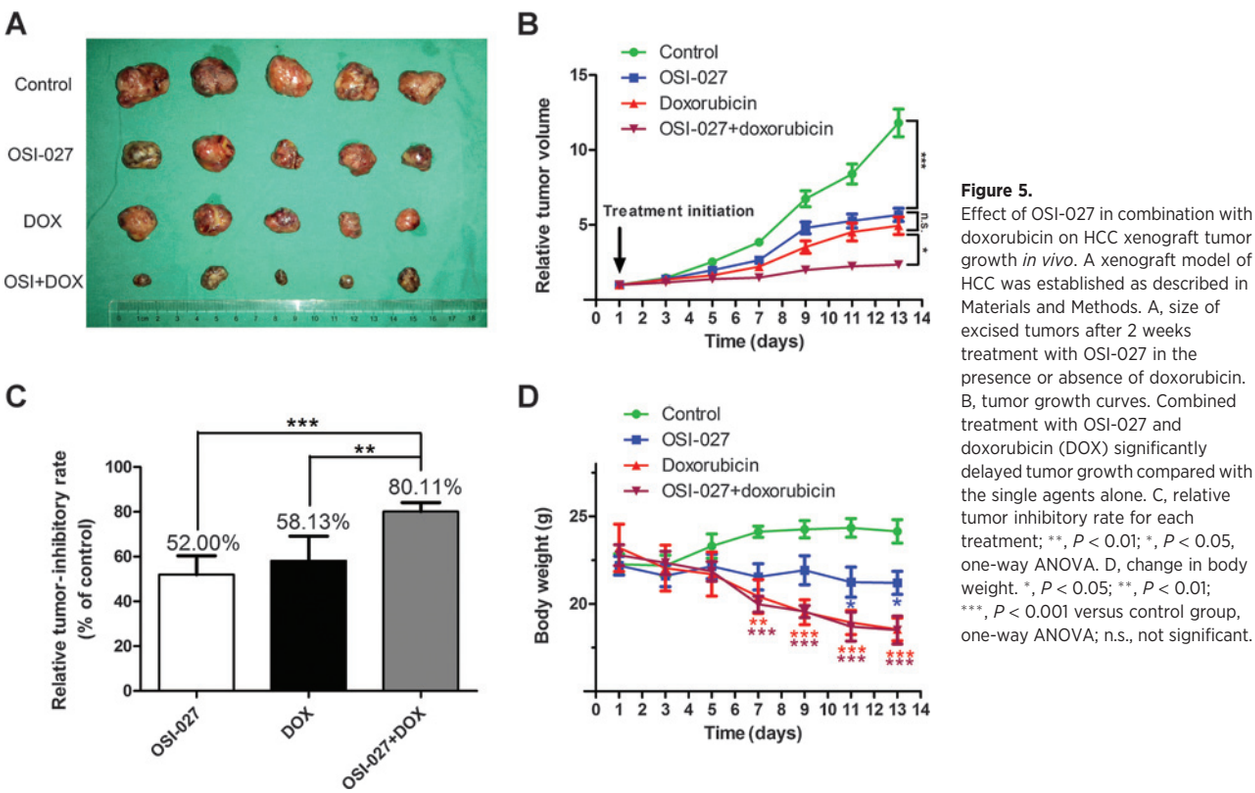

Figure 5.
Effect of OSI-027 in combination with doxorubicin on HCC xenograft tumor growth *in vivo*. A xenograft model of HCC was established as described in Materials and Methods. A, size of excised tumors after 2 weeks treatment with OSI-027 in the presence or absence of doxorubicin. B, tumor growth curves. Combined treatment with OSI-027 and doxorubicin (DOX) significantly delayed tumor growth compared with the single agents alone. C, relative tumor inhibitory rate for each treatment; **, $P < 0.01$; *, $P < 0.05$, one-way ANOVA. D, change in body weight. *, $P < 0.05$; **, $P < 0.01$; ***, $P < 0.001$ versus control group, one-way ANOVA; n.s., not significant.

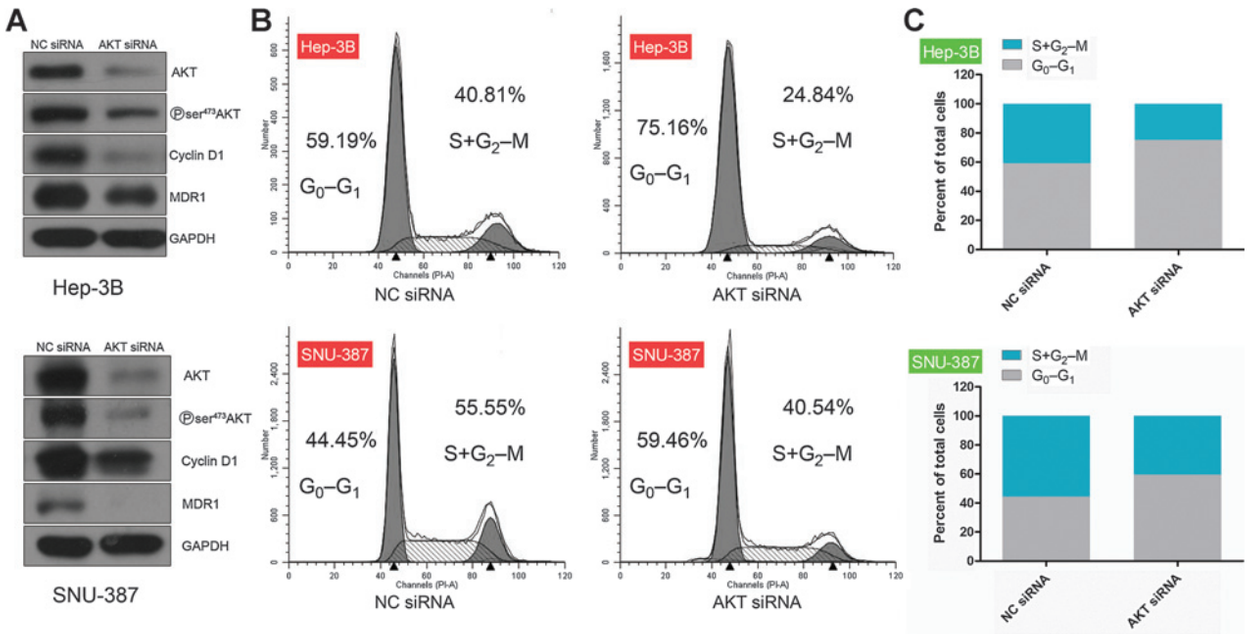

Figure 6.
Knockdown of *AKT* promotes G_0–G_1 arrest and downregulates MDR1. HCC cells were transfected with *AKT* or control (NC) siRNA. A, immunoblot analysis of p-AKT, MDR1, and cell-cycle–related markers for Hep-3B and SNU-387 cells; GAPDH was used as an internal loading control. B and C, flow-cytometric analysis (B) and quantification (C) of cell-cycle distribution.

of mTOR using rapamycin significantly reduces HCC and renal cell carcinoma xenograft tumor growth via exerting an anti-angiogenic effect (28, 39), and we previously reported that differentiation of monocytes into antitumor M1 macrophages may also participate in the antiangiogenic effect of rapamycin in HCC *in vivo* (42). In contrast, the present study demonstrated that all of the HCC cell lines tested were sensitive to the antiproliferative effects of mTORC1/mTORC2 inhibition using OSI-027. However, SNU-387 cells exhibited relatively low mTORC2 activity and decreased AKT phosphorylation on S473 (Fig. 2A), which may explain the lower sensitivity of this cell line to OSI-027.

We observed that OSI-027 did not induce apoptosis in HCC cells. OSI-027 induced apoptosis in only three of 22 various cell lines in one study and one of three bladder cancer cell lines in a separate study (19, 36), indicating that apoptosis is not a universal mode of action for this agent. However, inhibition of mTORC1/mTORC2 strongly induced apoptosis when combined with cytotoxic agents such as cisplatin or histone deacetylase inhibitors (17, 22), although we did not examine these combinations in HCC. However, these observations support the ability of mTOR inhibitors to promote apoptosis when administered with other drug combinations.

Targeted inhibition of mTORC2, but not mTORC1, potently prevented cells from transitioning from the G_0–G_1 phase to S phase (Fig. 3C–E). Further experiments demonstrated that AKT played a critical role in this complex process (Fig. 6). Numerous studies have demonstrated that mTORC2 regulates cell-cycle progression (43, 44); however, the precise mechanisms were poorly characterized. Previous studies reported that targeting mTORC2 suppresses Cyclin D1 translation via suppressing recruitment of Cyclin D1 mRNA to polysomes in acute myeloid leukemia and BCR-ABL–expressing chronic myeloid leukemia cells (45, 46). This mechanism is plausible, as the translational repressor 4E-BP1 that regulates cap-dependent mRNA translation is also deactivated by inhibition of mTORC2 (7, 8). However, decreased phosphorylation of AKT (S473) induced by inhibition of mTORC2 resulted in G_0–G_1 phase arrest and coincided with downregulation of Cyclin D1. Further investigation is urgently needed to elucidate the precise relationship between AKT and 4E-BP1 in cell-cycle progression.

The ability of hepatoma cells to become resistant to cytotoxic agents remains a significant hurdle to chemotherapy. Intrinsic or acquired multidrug resistances (MDR) are major causes of chemoresistance, especially to doxorubicin. The most extensively studied factor associated with MDR is increased expression of P-glycoprotein (also known as ABCB1 or MDR1; ref. 39), which is encoded by *MDR1*. Arceci and colleagues reported that rapamycin can reverse the MDR phenotype in human T-cell lymphoblastic leukemia cell lines (47), and increased activation of the PI3K/mTOR pathway was recently associated with overexpression of MDR1 in HCC (48). However, the effect of mTORC2 inhibition on MDR1 expression remained unknown. The present study demonstrates that OSI-027 reserves the overexpression of MDR1 induced by doxorubicin in HCC cells. Furthermore, inhibition of mTORC2 may mainly be responsible for this effect (Fig. 3E). We did not examine whether rapamycin exerts a similar effect on MDR1; however, knockdown of *Raptor* indicated that inhibition of mTORC1 alone had limited effect on MDR1 expression (Fig. 3E). These results indicate that PI3K/mTOR signaling regulates MDR1 via a number of mechanisms in different human cancer cells.

We then investigated how OSI-027 reduced the expression of MDR1. OSI-027 also downregulated *MDR1* mRNA expression (Fig. 4C), thus suppression of cap-dependent mRNA translation of the *MDR1* gene secondary to decreased phosphorylation

of 4E-BP1 cannot explain this observation. PI3K-AKT signaling regulates transcription of the *MDR1* gene. Silencing *AKT* demonstrated that OSI-027–induced downregulation of MDR1 was AKT dependent. AKT inhibitor was also introduced to further support this finding (Supplementary Fig. S8A and S8B). We also confirmed that AKT plays an essential role in transcription of *MDR1* (Supplementary Fig. S9). In agreement with our results, Kuo and colleagues reported that AKT activation induced *MDR1* mRNA expression in human HepG2 cells and human embryonic kidney (HEK)-293 cells via NF-κB signaling (49). Therefore, mTORC2 inhibition may suppress *MDR1* transcription by reducing AKT activity (Supplementary Fig. S10); further studies are needed to characterize this mechanism. In the present study, knockdown of *MDR1* significantly attenuated, but did not completely abrogate, the synergistic effect of OSI-027 and doxorubicin. First, siRNAs induce gene knockdown rather than complete gene knockout. Piguet and colleagues reported that temsirolimus sensitized HCC cells to DNA damage induced by doxorubicin via downregulating p21 (16), suggesting additional pathways may also sensitize HCC cells to doxorubicin.

Although current ATP-competitive mTOR inhibitors potently inhibit mTORC2 activity, they also perturb mTORC1-dependent negative feedback loops, which may limit the therapeutic potential of these agents. Moreover, knockdown of *Rictor* had less deleterious effects than knockdown of *Raptor* in mice skeletal muscle (50). To date, the relative significance of mTORC2 versus mTORC1 inhibition in cancer cell proliferation and chemoresistance remain unclear, and may vary in different cells. Therefore, mTORC2-specific inhibitors will prove useful for further preclinical research and may represent promising chemotherapeutic agents.

Disclosure of Potential Conflicts of Interest

No potential conflicts of interest were disclosed.

Authors' Contributions

Conception and design: B.W. Chen, W. Chen, C. Liang, X. Zhi, T.-B. Liang
Development of methodology: B.W. Chen, H. Liang, H. Liu, L.-Q. Hu, X.-Z. Yu, F. Xue
Acquisition of data (provided animals, acquired and managed patients, provided facilities, etc.): B.W. Chen, W. Chen, H. Liang, X. Zhi, L.-Q. Hu, T. Wei, L. Zheng, X.-L. Bai
Analysis and interpretation of data (e.g., statistical analysis, biostatistics, computational analysis): B.W. Chen, H. Liang, C. Liang, L.-Q. Hu, X.-Z. Yu, T. Wei, F. Xue, X.-L. Bai
Writing, review, and/or revision of the manuscript: B.W. Chen, W. Chen, H. Liang, B. Zhao, X-H. Feng, X.-L. Bai, T.-B. Liang
Administrative, technical, or material support (i.e., reporting or organizing data, constructing databases): H. Liu, X.-Z. Yu, T. Ma, B. Zhao
Study supervision: H. Liu, T. Ma, T.-B. Liang

Grant Support

This work was supported by the National High Technology Research and Development Program 863 of China (SS2014AA020534; to W. Chen), the National Key Basic Research Program of China (2014CB542101, to T.-B. Liang; 2012CB966600, to X.H. Feng), the National Natural Science Foundation of China (81472212, to T.-B. Liang; 81302071, to W. Chen; 81171884, to X.L. Bai; 81273260, to F. Xue; and 31090360, to X.H. Feng), the National Natural Science Funds for Distinguished Young Scholar of China (30925033, to T.-B. Liang), Project 111 (to X.H. Feng), Project 985 (to X.H. Feng), and the Innovation and High-Level Talent Training Program of Department of Health of Zhejiang (to T.-B. Liang).

The costs of publication of this article were defrayed in part by the payment of page charges. This article must therefore be hereby marked *advertisement* in accordance with 18 U.S.C. Section 1734 solely to indicate this fact.

Received January 29, 2015; revised May 4, 2015; accepted May 17, 2015; published OnlineFirst May 29, 2015.

References

1. Jemal A, Bray F, Center MM, Ferlay J, Ward E, Forman D. Global cancer statistics. CA Cancer J Clin 2011;61:69–90.
2. Lin S, Hoffmann K, Schemmer P. Treatment of hepatocellular carcinoma: a systematic review. Liver Cancer 2012;1:144–58.
3. Park SH, Lee Y, Han SH, Kwon SY, Kwon OS, Kim SS, et al. Systemic chemotherapy with doxorubicin, cisplatin and capecitabine for metastatic hepatocellular carcinoma. BMC Cancer 2006;6:3.
4. Yeo W, Mok TS, Zee B, Leung TW, Lai PB, Lau WY, et al. A randomized phase III study of doxorubicin versus cisplatin/interferon a-2b/doxorubicin/fluorouracil(PIAF) combination chemotherapy for unresectable hepatocellular carcinoma. J Natl Cancer Inst 2005;97:1532–8.
5. Schwartz JD, Schwartz M, Mandeli J, Sung M. Neoadjuvant and adjuvant therapy for resectable hepatocellular carcinoma: review of the randomised clinical trials. Lancet Oncol 2002;3:593–603.
6. Bjornsti MA, Houghton PJ. The TOR pathway: a target for cancer therapy. Nat Rev Cancer 2004;4:335–48.
7. Tamburini J, Green AS, Bardet V, Chapuis N, Park S, Willems L, et al. Protein synthesis is resistant to rapamycin and constitutes a promising therapeutic target in acute myeloid leukemia. Blood 2009;114:1618–27.
8. Gingras AC, Gygi SP, Raught B, Polakiewicz RD, Abraham RT, Hoekstra MF, et al. Regulation of 4E-BP1 phosphorylation: a novel two-step mechanism. Genes Dev 1999;13:1422–37.
9. Sarbassov DD, Guertin DA, Ali SM, Sabatini DM. Phosphorylation and regulation of Akt/PKB by the rictor-mTOR complex. Science 2005;307:1098–101.
10. Laplante M, Sabatini DM. mTOR signaling in growth control and disease. Cell 2012;149:274–93.
11. Loewith R, Jacinto E, Wullschleger S, Lorberg A, Crespo JL, Bonenfant D, et al. Two TOR complexes, only one of which is rapamycin sensitive, have distinct roles in cell growth control. Mol Cell 2002;10:457–68.
12. Copp J, Manning G, Hunter T. TORC-specific phosphorylation of mammalian target of rapamycin (mTOR): phospho-Ser2481 is a marker for intact mTOR signaling complex 2. Cancer Res 2009;69:1821–7.
13. Sahin F, Kannangai R, Adegbola O, Wang J, Su G, Torbenson M. mTOR and P70 S6 kinase expression in primary liver neoplasms. Clin Cancer Res 2004;10:8421–5.
14. Villanueva A, Chiang DY, Newell P, Peix J, Thung S, Alsinet C, et al. Pivotal role of mTOR signaling in hepatocellular carcinoma. Gastroenterology 2008;135:1972–83.
15. Tam KH, Yang ZF, Lau CK, Lam CT, Pang RW, Poon RT. Inhibition of mTOR enhances chemosensitivity in hepatocellular carcinoma. Cancer Lett 2009;273:201–9.
16. Piguet AC, Semela D, Keogh A, Wilkens L, Stroka D, Stoupis C, et al. Inhibition of mTOR in combination with doxorubicin in an experimental model of hepatocellular carcinoma. J Hepatol 2008;49:78–87.
17. Shao H, Gao C, Tang H, Zhang H, Roberts LR, Hylander BL, et al. Dual targeting of mTORC1/C2 complexes enhances histone deacetylase inhibitor-mediated anti-tumor efficacy in primary HCC cancer *in vitro* and *in vivo*. J Hepatol 2012;56:176–83.
18. Wan X, Harkavy B, Shen N, Grohar P, Helman L. Rapamycin induces feedback activation of Akt signaling through an IGF-1R-dependent mechanism. Oncogene 2007;26:1932–40.
19. Bhagwat SV, Gokhale PC, Crew AP, Cooke A, Yao Y, Mantis C, et al. Preclinical characterization of OSI-027, a potent and selective inhibitor of mTORC1 and mTORC2: distinct from rapamycin. Mol Cancer Ther 2011;10:1394–406.
20. Falcon BL, Barr S, Gokhale PC, Chou J, Fogarty J, Depeille P, et al. Reduced VEGF production, angiogenesis, and vascular regrowth contribute to the antitumor properties of dual mTORC1/mTORC2 inhibitors. Cancer Res 2011;71:1573–83.

21. Gupta M, Hendrickson AE, Yun SS, Han JJ, Schneider PA, Koh BD, et al. Dual mTORc1/mTORc2 inhibition diminishes AKT activation and induces PUMA-dependent apoptosis in lymphoid malignancies. Blood 2012;119: 476–87.
22. Li H, Lin J, Wang X, Yao G, Wang L, Zheng H, et al. Targeting of mTORC2 prevents cell migration and promotes apoptosis in breast cancer. Breast Cancer Res Treat 2012;134:1057–66.
23. Cassell A, Freilino ML, Lee J, Barr S, Wang L, Panahandeh MC, et al. Targeting TORC1/2 enhances sensitivity to EGFR inhibitors in head and neck cancer preclinical models. Neoplasia 2012;14:1005–14.
24. Kirstein MM, Boukouris AE, Pothiraju D, Buitrago-Molina LE, Marhenke S, Schütt J, et al. Activity of the mTOR inhibitor RAD001, the dual mTOR and PI3-kinase inhibitor BEZ235 and the PI3-kinase inhibitor BKM120 in hepatocellular carcinoma. Liver Int 2013;33:780–93.
25. Camplejohn RS. Flow cytometric measurement of cell proliferation. Methods Mol Med 2001;57:133–43.
26. Chou TC. Theoretical basis, experimental design, and computerized simulation of synergism and antagonism in drug combination studies. Pharmacol Rev 2006;58:621–81.
27. Livak KJ, Schmittgen TD. Analysis of relative gene expression data using real-time quantitative PCR and the 2(-Delta Delta C(T)) Method. Methods 2001;25:402–8.
28. Semela D, Piguet AC, Kolev M, Schmitter K, Hlushchuk R, Djonov V, et al. Vascular remodeling and antitumoral effects of mTOR inhibition in a rat model of hepatocellular carcinoma. J Hepatol 2007;46:840–8.
29. Salic A, Mitchison TJ. A chemical method for fast and sensitive detection of DNA synthesis in vivo. Proc Natl Acad Sci U S A 2008;105:2415–20.
30. Feldman ME, Apsel B, Uotila A, Loewith R, Knight ZA, Ruggero D, et al. Active-site inhibitors of mTOR target rapamycin-resistant outputs of mTORC1 and mTORC2. PLoS Biol 2009;7:0371–83.
31. Choo AY, Yoon SO, Kim SG, Roux PP, Blenis J. Rapamycin differentially inhibits S6Ks and 4E-BP1 to mediate cell-type-specific repression of mRNA translation. Proc Natl Acad Sci U S A 2008;105:17414–9.
32. Faivre S, Kroemer G, Raymond E. Current development of mTOR inhibitors as anticancer agents. Nat Rev Drug Discov 2006;5:671–88.
33. Guertin DA, Sabatini DM. Defining the role of mTOR in cancer. Cancer Cell 2007;12:9–22.
34. Wullschleger S, Loewith R, Hall MN. TOR signaling in growth and metabolism. Cell 2006;124:471–84.
35. Meric-Bernstam F, Gonzalez-Angulo AM. Targeting the mTOR signaling network for cancer therapy. J Clin Oncol 2009;27:2278–87.
36. Becker MN, Wu KJ, Marlow LA, Kreinest PA, Vonroemeling CA, Copland JA, et al. The combination of an mTORc1/TORc2 inhibitor with lapatinib is synergistic in bladder cancer *in vitro*. Urol Oncol 2014;32: 317–26.
37. Hara K, Maruki Y, Long X, Yoshino K, Oshiro N, Hidayat S, et al. Raptor, a binding partner of target of rapamycin (TOR), mediates TOR action. Cell 2002;110:177–89.
38. Jacinto E, Facchinetti V, Liu D, Soto N, Wei S, Jung SY, et al. SIN1/MIP1 maintains rictor-mTOR complex integrity and regulates Akt phosphorylation and substrate specificity. Cell 2006;127:125–37.
39. Park JG, Lee SK, Hong IG, Kim HS, Lim KH, Choe KJ, et al. MDR1 gene expression: its effect on drug resistance to doxorubicin in human hepatocellular carcinoma celllines. J Natl Cancer Inst 1994;86:700–5.
40. Katayama K, Noguchi K, Sugimoto Y. FBXO15 regulates P-glycoprotein/ABCB1 expression through the ubiquitin proteasome pathway in cancer cells. Cancer Sci 2013;104:694–702.
41. Oudard S, Medioni J, Aylllon J, Barrascourt E, Elaidi RT, Balcaceres J, et al. Everolimus (RAD001): an mTOR inhibitor for the treatment of metastatic renal cell carcinoma. Expert Rev Anticancer Ther 2009;9:705–17.
42. Chen W, Ma T, Shen XN, Xia XF, Xu GD, Bai XL, et al. Macrophage-induced tumor angiogenesis is regulated by the TSC2-mTOR pathway. Cancer Res 2012;72:1363–72.
43. Masri J, Bernath A, Martin J, Jo OD, Vartanian R, Funk A, et al. mTORC2 activity is elevated in gliomas and promotes growth and cell motility via overexpression of rictor. Cancer Res 2007;67:11712–20.
44. Smrz D, Kim MS, Zhang S, Mock BA, Smrzová S, DuBois W, et al. mTORC1 and mTORC2 differentially regulate homeostasis of neoplastic and non-neoplastic human mast cells. Blood 2011;118:6803–13.
45. Carayol N, Vakana E, Sassano A, Kaur S, Goussetis DJ, Glaser H, et al. Critical roles for mTORC2- and rapamycin-insensitive mTORC1-complexes in growth and survival of BCR-ABL-expressing leukemic cells. Proc Natl Acad Sci U S A 2010;107:12469–74.
46. Altman JK, Sassano A, Kaur S, Glaser H, Kroczynska B, Redig AJ. Dual mTORC2/mTORC1 targeting results in potent suppressive effects on acute myeloid leukemia (AML) progenitors. Clin Cancer Res 2011;17:4378–88.
47. Arceci RJ, Stieglitz K, Bierer BE. Immunosuppressants FK506 and rapamycin function as reversal agents of the multidrug resistance phenotype. Blood 1992;80:1528–36.
48. Wang SF, Chou YC, Mazumder N, Kao FJ, Nagy LD, Guengerich FP, et al. 7-Ketocholesterol induces P-glycoprotein through PI3K/mTOR signaling in hepatoma cells. Biochem Pharmacol 2013;86:548–60.
49. Kuo MT, Liu Z, Wei Y, Lin-Lee YC, Tatebe S, Mills GB, et al. Induction of human MDR1gene expression by 2-acetylaminofluorene is mediated by effectors of the phosphoinositide 3-kinase pathway that activate NF-kB signaling.Oncogene 2002;21:1945–54.
50. Bentzinger CF, Romanino K, Cloëtta D, Lin S, Mascarenhas JB, Oliveri F, et al. Skeletal muscle-specific ablation of raptor, but not of rictor, causes metabolic changes and results in muscle dystrophy. Cell Metab 2008;8: 411–24.